Volume and Enthalpy Changes after Photoexcitation of Bovine Rhodopsin: Laser-Induced Optoacoustic Studies

Julia M. Strassburger, Wolfgang Gärtner, and Silvia E. Braslavsky
Max-Planck-Institut für Strahlenchemie, D-45413 Mülheim an der Ruhr, Germany

ABSTRACT Laser-induced optoacoustic measurements were performed with bovine rhodopsin in the temperature range 5–32°C in its natural environment (i.e., in washed membranes) as well as solubilized in dodecyl-β-D-maltoside. A signal deconvolution procedure using a simple sequential kinetic scheme for the photobaric time evolution revealed, in the case of the washed membranes, the presence of an intermediate with a 14-ns lifetime at 25°C, of the same order as that reported for the BSI intermediate in solubilized rhodopsin (Hug, S. J., W. J. Lewis, C. M. Einterz, T. E. Thorgeirsson, and D. S. Kliger. 1990. Nanosecond photolysis of rhodopsin: evidence for a new, blue-shifted intermediate. *Biochemistry*. 29:1475–1485), with an energy content of (85 ± 20) kJ/mol, and accompanied by an expansion of 26 ± 3 ml/mol. The difference in energy content between BSI and the next transient lumi was estimated in only −1 ± 5 kJ/mol, concomitant with an expansion of 9 ± 3 ml/mol. Thus, this transition, which according to literature involves an equilibrium, should be controlled by an entropic change, rather than by an enthalpic difference. This is supported by the fact that both activation parameters for the decay of batho and BSI decrease upon solubilization. For detergent-solubilized rhodopsin, two time constants were enough to fit the sample signal. A short lifetime ascribable to BSI was not detected in this case. For the first intermediate (probably batho in equilibrium with BSI), an energy content of 50 ± 20 kJ/mol and an expansion of 20 ± 1 ml/mol, and for lumi an energy content of 11 ± 20 kJ/mol and a further expansion of 11 ± 2 ml/mol were determined. Thus, the intermediates of the membrane-embedded form of rhodopsin (in contrast to solubilized samples) are kept in a higher energy level, although the total expansion from rhodopsin to lumi is similar for both conditions (35 ± 6 and 31 ± 3 ml/mol). The expansions are interpreted as protein reorganization processes as a consequence of the photoisomerization of the chromophore. As a result, weak interactions are probably perturbed and the protein gains conformational flexibility.

INTRODUCTION

The visual pigment rhodopsin, located in the outer segments of the visual cells, is the first component of the light-induced visual transduction cascade (Hargrave et al., 1993). It belongs to the large protein family of G-protein-coupled receptors which share the structural motif of seven membrane-spanning α-helices (Ovchinnikov, 1982; Baldwin, 1993; Schertler et al., 1993; Strader et al., 1994). Rhodopsin is activated upon the photoisomerization of its covalently bound chromophore 11-*cis* retinal into the all-*trans* configuration. This highly efficient photoreaction (quantum yield, $\Phi = 0.67$, Dartnall, 1972) is complete within <1 ps (Schoenlein et al., 1991) and produces a first photointermediate, bathorhodopsin (batho). The energy stored in the batho intermediate has been estimated between 109 and 146 kJ/mol (for a review see Birge, 1990) using calorimetric techniques either at low temperature (Cooper, 1981) or with dried rod outer segments (Boucher and Leblanc, 1985). This value indicates that ~60% of the absorbed photon energy is stored in the first transient. Subsequently, a series of exergonic conformational changes of the protein and the chromophore occur, extending into the time range of several seconds, and eventually leading to the release of the chromophore, i.e., the irreversible bleaching of rhodopsin. The formation of the physiologically active intermediate metarhodopsin II, which activates the G-protein, takes place within several milliseconds in this reaction sequence (Hofmann, 1995).

The conformational changes become evident by changes of the absorption of rhodopsin (λ_{max} = 500 nm) and have been investigated by several spectroscopic techniques, among which UV/vis absorption and vibrational spectroscopy (FTIR and resonance Raman) have provided the most detailed structural information (Palings et al., 1987; Mizukami et al., 1993; Rothschild and DeGrip, 1992; García-Quintana et al., 1995; Kliger and Lewis, 1995). Open questions remain about the energy content of the various intermediates, especially under physiological environment conditions, and about the protein movements taking place during the transformation.

In addition to the well-known intermediates of the rhodopsin conversion, which are batho (λ_{max} = 540 nm), lumi (λ_{max} = 497 nm), metarhodopsin I (λ_{max} = 478 nm), and metarhodopsin II (λ_{max} = 380 nm), detailed analysis of optical data has revealed the presence of a blue-shifted intermediate (BSI) formed from batho which decays into lumi (Hug et al., 1990; Kliger and Lewis, 1995) (Fig. 1). Hug et al. proposed an equilibrium between batho and BSI instead of a parallel model with two batho intermediates decaying to one or more lumi products.

Received for publication 1 July 1996 and in final form 5 February 1997.
Address reprint requests to Professor Dr. Silvia E. Braslavsky, Max-Planck-Institut für Strahlenchemie, Postfach 101365, Stiftstrasse 34-36, D-45413 Mülheim an der Ruhr, Germany. Tel.: 49-208-306-3681 (direct), 49-208-306-0 (switchboard); Fax: 49-208-306-3951; Internet: braslavskys@mpi-muelheim.mpg.de.

0006-3495/97/05/2294/10 $2.00

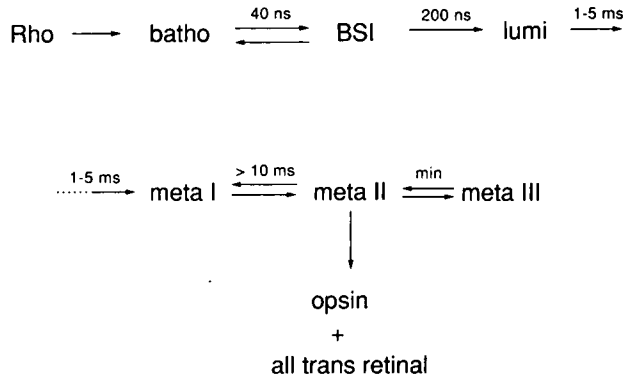

FIGURE 1 Simplified reaction scheme describing the events in the first microseconds following excitation of rhodopsin. Modified after Hofmann (1995) and Kliger and Lewis (1995). The time constants of 40 and 200 ns are the apparent decay times of batho and BSI at ambient temperature in solubilized rhodopsin.

The enthalpy changes taking place during the stepwise photoinduced transformation of rhodopsin, and the structural volume changes of the chromophore and its surroundings associated with the transformation, contribute to the pressure signal detected by photobaric methods such as photoacoustics (Callis et al., 1972) and time-resolved laser-induced optoacoustic spectroscopy (LIOAS) (Peters and Snyder, 1988; Braslavsky and Heibel, 1992; Crippa et al., 1994). Since the LIOAS signal generation due to heat release depends on the thermoelastic parameters of the solution, while the signal originating from structural volume changes does not, LIOAS measurements at various temperatures in aqueous solutions of photoreceptors permit the separation of the thermal from the structural volume contribution to the pressure pulse. This approach has been used to time-resolve the enthalpy and structural volume changes taking place during several microseconds after excitation of various biological photoreceptors (Schulenberg and Braslavsky, 1997). In particular, photoreceptors bearing an isomerizable chromophore, such as phytochrome and the photoactive yellow protein, can advantageously be analyzed by this technique (Gensch et al., 1996; van Brederode et al., 1995). In these cases, the structural volume changes determined were associated with the changes in the surrounding protein induced by the photoisomerization of the respective chromophore.

Bovine rhodopsin has also been studied by LIOAS at several temperatures (Marr and Peters, 1991). However, due to the long integration time (1.3 μs) of these experiments, the authors could not time-resolve the changes even by using deconvolution techniques. Using solubilized rhodopsin, these authors reported a total structural volume change of 29 ml/mol for the transition rhodopsin $\rightarrow$ lumi and a corresponding enthalpy step of 227.4 kJ/mol, after excitation with 500 nm leaving the transient lumi with an energy content of 16 kJ/mol.

The time-dependent behavior of the processes under inspection with LIOAS can be followed down to several nanoseconds by applying appropriate deconvolution procedures to fit the signals (Rudzki-Small, 1992; Crippa et al., 1994). For systems in which transients with relatively long lifetimes or stable products are produced, there is no need to use this fitting procedure. However, in the rhodopsin case deconvolution should be used in a similar manner as applied to other systems in our laboratory (Habib-Jiwan et al., 1995) with due consideration of the kinetic scheme under analysis.

Thus, LIOAS permits the study of the kinetics of photoinduced processes with photoreceptors in which optical measurements are impaired by the fact that the absorption spectra of the intermediates overlap with that of the ground state and by a high scattering due to the membrane-intrinsic nature of the chromoproteins.

In this contribution we present time-resolved LIOAS measurements in the temperature range of 5–32°C with bovine rhodopsin in washed membranes, i.e., in the natural environment of the visual pigment, as well as solubilized with the nonionic detergent dodecyl-β-D-maltoside. Using a detailed kinetic analysis and a deconvolution procedure, we take into account the participation of several intermediates in the time range from 20 ns to several microseconds. The use of two different detectors, i.e., a ceramic piezoelement at the lower temperatures (at which the signals are smaller) and a film detector at the higher temperatures (at which the signals are faster) allowed the analysis in a relatively large temperature range and the description of the photochemistry of rhodopsin with detailed information on the time course of the enthalpy and the structural volume changes in the time range of several microseconds after the 15-ns laser pulse.

MATERIALS AND METHODS

Isolation of washed membranes and sample handling

The preparation of washed membranes was carried out at 4°C and under dim red light using an RG-650 filter (Schott). The isolation of the rhodopsin-containing washed membranes from fresh bovine eyes was performed according to DeGrip et al. (1980). All measurements were performed in Ringer's solution (130 mM KCl, 10 mM Pipes, 1 mM DTT, 1 mM $CaCl_2 \cdot 6H_2O$, 0.5 mM EDTA, 0.5 mM $MgCl_2 \cdot 6H_2O$, 0.1 mM PMSF, pH 7.0) with sample concentrations of ~5 μM in a 3.5-ml 1 × 1 cm quartz cuvette. The absorbance at 500 nm, A_{500} = 0.7, included scattering of ~0.5–0.6, depending on the sample. Bleached washed membranes used for the determination of the reference signal were obtained by exhaustively irradiating with white light an aliquot of the sample membrane suspension used for the measurements.

For solubilization of rhodopsin, a 2% dodecyl-β-D-maltoside (Boehringer Mannheim) Ringer's solution was used. After gentle shaking overnight at 4°C, the sample was centrifuged at $10^5 \times g$ for 1 h. The supernatant was used for the LIOAS measurements. For these measurements, Evans blue was used as calorimetric reference. The reference measurements were performed in the presence of bleached solubilized rhodopsin.

Absorption spectroscopy

Absorption spectra were recorded with a 2102-PC UV/vis spectrophotometer (Shimadzu, Columbia, MD) or with a Perkin-Elmer 356 UV/vis

spectrophotometer with a sample compartment near a head-on photomultiplier, allowing measurements of strongly scattering samples. This permitted a precise determination of the absorbance due only to rhodopsin, i.e., without scattering.

Laser-induced optoacoustic spectroscopy (LIOAS)

The LIOAS system has already been described elsewhere (Braslavsky and Heibel, 1992; Churio et al., 1994). Briefly, the 15-ns pulses from an excimer laser (EMG 101 MSG, Lambda Physik, Göttingen), λ_{exc} = 308 nm were used to pump a dye laser system (FL 2000, Lambda Physik) using Coumarin 307 (λ_{em} = 500 nm; Radiants Dyes Chemie). The pulse total energy was varied using an attenuator and measured with a pyroelectric energy meter (Laser Precision Corp. RJP735 head connected to a RJ7100 meter). The laser energy range was 5–15 μJ per pulse, which resulted in a linear relationship between excitation energy and LIOAS signal amplitude. The total energy was adjusted to similar values for reference and sample. Before passing through the sample, the laser beam was widened using a telescope with a magnification of 5 and shaped by a slit (0.5 × 8 mm or 0.8 × 8 mm). The acoustic transit time was then between ~330 and 530 ns (Braslavsky and Heibel, 1992).

The pressure wave was detected at a cuvette wall parallel to the direction of the exciting beam with either a 4-mm piezoelectric Pb-Zr-Ti ceramic or a piezoelectric polyvinyl difluoride foil (PVF_2; 40 μm thickness). The detector was firmly fixed to the side wall of the quartz cuvette (Heihoff et al., 1987; Braslavsky and Heihoff, 1989). The temperature range used was 5–32°C. The temperature regulation was ±0.1°C.

Taking into account the faster kinetics at the higher temperatures, i.e., 25 and 32°C, the foil was used for detection allowing for better time resolution (10–15 ns). For the observation of the same processes at lower temperatures, i.e., 5, 10, and 12°C (lifetimes of several hundreds of nanoseconds), the ceramic transducer was chosen due to its higher sensitivity (Braslavsky and Heihoff, 1989). The resulting signal was digitized and averaged by a Tektronix 520A oscilloscope with 2 ns/channel resolution, and then transferred to a VAX station 3100. Deconvolution was performed with the Sound Analysis 3000 program (Quantum Northwest) on a PC.

For each LIOAS measurement at one temperature and one laser fluence the average of 60–80 single flashes was needed, which caused a net bleaching of the rhodopsin sample of <10%. The sample was stirred after each laser pulse. A fresh sample was always provided before the onset of the next LIOAS series. By the largest fluences used, a value of only 0.1 photon/molecule was reached.

Bromocresol purple (BCP, Sigma) and Evans blue (Aldrich) served as calorimetric references. To account for the scattering properties of the rhodopsin samples in washed membranes or in dodecyl-β-D-maltoside, reference measurements were performed in Ringer's solution containing bleached washed membranes or bleached solubilized rhodopsin, respectively, in the same amount as the respective sample. The cuvette wall to which the detector was attached was externally silvered. This notably decreased the effect of light scattering in the signal shape.

For the determination of the thermoelastic parameters in the Ringer's solution with bleached washed membranes, Evans blue as a calorimetric reference was excited with the pulses of a Nd:YAG-pumped dye laser at 650 nm (DCM dye) (Gensch et al., 1996). A wide pinhole affording an acoustic transit time of 1.5 μs was used for the determination of the thermoelastic parameters to minimize the influence of scattering. In the case of the detergent-containing Ringer's solution, excitation of Evans blue was at 500 nm and the signal was compared to that of Evans blue in neat water.

Densities were measured using density hydrometers (Fleischhacker, Germany) and compared to that of water at the same temperature.

RESULTS AND DISCUSSION

The reference system

In all cases known, retinal (photo)receptors are found as intrinsic membrane proteins. This property impairs the investigation in the native surrounding by optical methods due to the high light scattering by the samples. Light scattering also has an impact on LIOAS since it alters the shape and the amplitude of the signals. This effect becomes critical for a deconvolution procedure and for small signal amplitudes, since reference and sample should exhibit nearly identical absorption properties (Nitsch et al., 1988). To reduce the effect of scattering, in addition to silvering the wall of the cuvette to which the detector was attached, we took advantage of the irreversible bleaching of rhodopsin: the calorimetric reference was measured in a bleached aliquot of the sample suspension both in the case of the washed membranes as in the solubilized rhodopsin; this allowed a direct comparison of the signal shape for reference and sample. This also enabled, for the case of the washed membranes, the analysis of the protein in its native membrane surrounding. To analyze the effect of solubilization we also performed measurements with solubilized rhodopsin, since it is known that solubilization and the detergent affect the later equilibrium meta I⇆ meta II (Lamola et al., 1974; Applebury et al., 1974; König et al., 1989).

The added salts, the detergent, and the membrane content change the thermoelastic parameters ($c_p\rho/\beta$; with c_p = heat capacity, ρ = density, and β = volume expansion coefficient) with respect to the values for neat water. To determine the new parameters, we compared the LIOAS signal amplitudes for Evans blue in water to those in Ringer's solution (pH 7.0) containing bleached washed membranes at temperatures from 5 to 32°C (see Fig. 2), and to those in Ringer's solution containing detergent and bleached rhodopsin. Since the LIOAS signal amplitude is proportional to

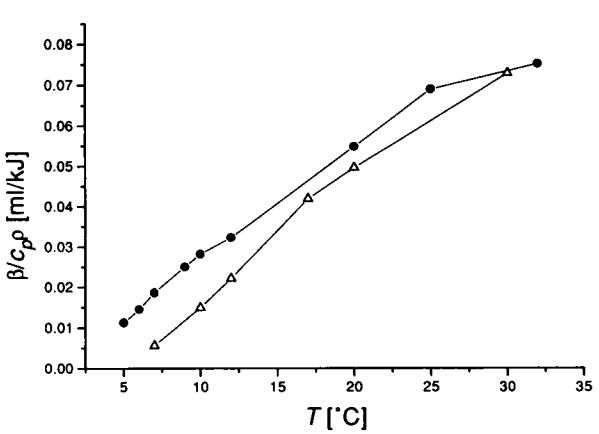

FIGURE 2 Temperature dependence of $\beta/c_p\rho$ (●) for a Ringer's solution in the presence of washed membranes, λ_{exc} = 650 nm, and (△) for a Ringer's solution containing 2% dodecyl-β-D-maltoside and bleached rhodopsin, λ_{exc} = 500 nm. In both cases Evans blue served as a calorimetric reference. A relatively large integration time of ~1.5 μs was used.

the compressibility in addition to $\beta/c_p\rho$, it was necessary to compare the density ρ and the sound velocity v_a of the medium (as determined from the acoustic wave arrival time) to the known values of water. The difference was negligible, as already found for other systems (Churio et al., 1994; Habib-Jiwan et al., 1995; Gensch et al., 1996). Thus, the ratios of the fluence-normalized LIOAS amplitudes for the reference in water and in the investigated medium, determined at each temperature, afforded the $c_p\rho/\beta$ values either for the washed membranes in Ringer's solution or for the detergent-containing medium (Fig. 2).

Deconvolution analysis

The procedure for deconvolution of the signals was as described by Rudzki-Small (1992) and by Crippa et al. (1994). The acoustic signal $S(t)$ can be regarded as a convolution between instrument response $R(t)$ and a time-dependent pressure evolution $P(t)$ (Eq. 1)

$$S(t) = R(t) \otimes P(t) \tag{1}$$

The calorimetric reference system delivers all the absorbed energy to the medium as prompt heat (apparent amplitude, $\varphi^{app} = 1$, Eq. 2), i.e., within a time shorter than the time resolution of the experiment. $R(t)$ is thus the signal of the reference. After convolution, the resulting simulated signal is compared to the measured sample waveform and a minimization of the differences between signal and simulated function (χ^2 values) is searched for by the program.

$$P(t) = \sum_i \frac{\varphi_i^{app}}{\tau_i} \exp(-t/\tau_i) \tag{2}$$

The measured (apparent) amplitudes, φ_i^{app}, of the fitting function (Eq. 2) are related to the observed decay lifetimes τ_i. Only in the case of parallel unimolecular processes, or sequential processes with lifetimes differing by about one order of magnitude or more, the φ_i^{app} values correspond in a simple manner to the parameters of the elementary steps. This is not so in the rhodopsin case.

To relate the φ_i^{app} values to the parameters of the elementary steps in the sequential rhodopsin phototransformation mechanism, the following set of equations (3–5) were used (Rudzki-Small, 1992). As a first approximation, a purely sequential analysis was used without taking into account equilibria between transients.

$$\varphi_3 = \varphi_3^{app} \frac{(\tau_3 - \tau_1)(\tau_3 - \tau_2)}{\tau_3^2} \tag{3}$$

$$\varphi_2 = \varphi_2^{app} \frac{\tau_2 - \tau_1}{\tau_2} + \varphi_3 \frac{\tau_2}{\tau_3 - \tau_2} \tag{4}$$

$$\varphi_1 = \varphi_1^{app} + \varphi_2 \frac{\tau_1}{\tau_2 - \tau_1} + \varphi_3 \frac{\tau_1^2}{(\tau_3 - \tau_1)(\tau_1 - \tau_2)} \tag{5}$$

The values φ_1, φ_2, and φ_3 represent the weight of each elementary process (subscript 1 for the production of batho, 2 for the batho to BSI, and 3 for the BSI to lumi process) to the total LIOAS signal. Equation 6 shows the relationship between the amplitudes φ_i and the thermoelastic parameters ($c_p\rho/\beta$), whereby β is strongly temperature-dependent in neat water and in aqueous solutions. This equation is based on the observation by Callis et al. (1972) that the photoinduced pressure pulse in an absorbing system may be due to 1) the heat release and 2) the volume change concomitant with the monitored step, and on the assumption that in a given reaction step the time-dependence of the heat delivered by radiationless processes is the same as that of concomitant structural volume changes.

$$\varphi_i E_\lambda = q_i + \Phi_i \Delta V_{R,i}(c_p\rho/\beta) \tag{6}$$

In Eq. 6 E_λ is the molar laser energy, q_i is the fraction of evolved heat for the ith process, $\Delta V_{R,i}$ is the volume change during the formation of transient i per converted mol, and Φ_i is the corresponding quantum yield. By using Eq. 6, the volume change for each process, $\Delta V_{R,i}$, is calculated from the slope of a plot depicting φ_i at various temperatures (variable $c_p\rho/\beta$). The heat released during each step, q_i, is determined from the intercept of such a plot.

The lifetimes

An example of a deconvolution between the signal for washed membranes and the reference at 10°C using a ceramic detector is shown in Fig. 3 *a*, and one with a PVF_2 film at 25°C in Fig. 3 *b*.

The quality of the fit was judged by a low χ^2 value and a visual inspection of the residuals distribution (see, e.g., Fig. 3), as well as by their autocorrelation function (Rudzki-Small, 1992). The fitting procedure yields preexponential φ_i^{app} factors and the corresponding lifetimes τ_i.

The number of observable lifetimes in the washed membranes suspensions was different from the number for solubilized protein. In the former case, the fitting procedure delivered three apparent lifetimes, while in the latter case only two lifetimes were observed. In Fig. 3 *c* it is shown that a fitting with a three-exponential function did not bring an improvement of the residuals distribution. For both conditions, the very fast lifetime τ_1 with its amplitude φ_1 is related to the sum of nonradiative processes (such as internal conversion) plus vibrational relaxations as well as the initial isomerization, i.e., the fast rise of the batho intermediate. This lifetime is shorter than the time resolution of the experiment. Fixing this parameter at any value <1 ns always resulted in a similar value for the associated amplitude of that process. This is in agreement with a report on the formation of batho within <1 ps (Peteanu et al., 1993). The other observed lifetimes τ_2 and τ_3, in the case of the washed membranes, should be related to the subsequent processes of the rhodopsin photoconversion, i.e., batho decay to BSI followed by the decay of BSI to lumi (as reported by Hug et al., 1990, for solubilized rhodopsin) (Table 1). Solubilized

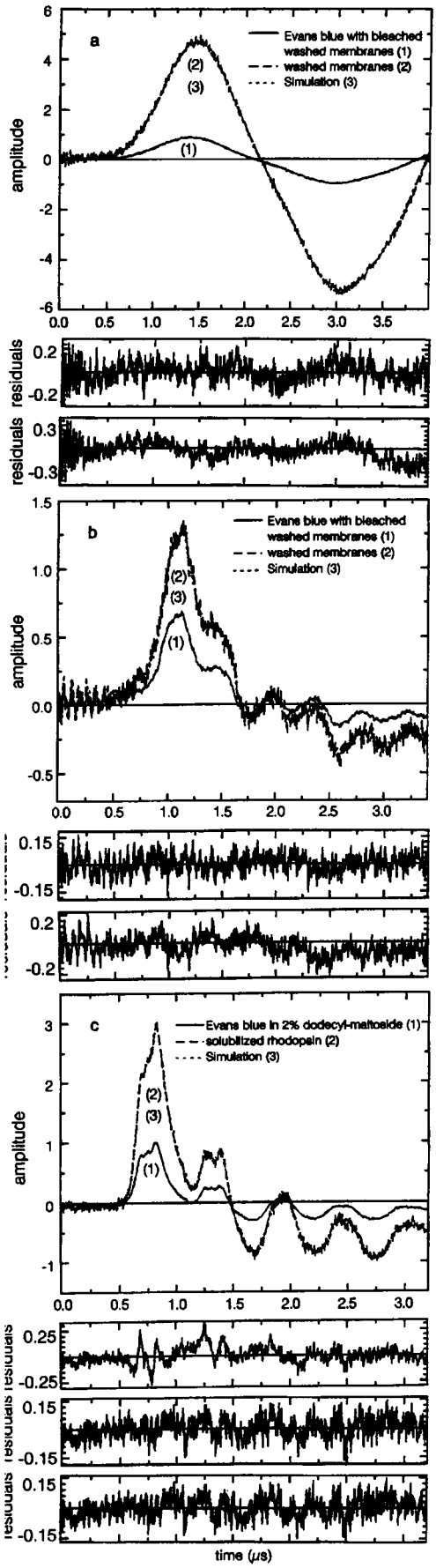

TABLE 1 Lifetimes derived from the deconvolution procedure of the LIOAS signals in the temperature range 5–32°C for washed membranes (τ_1 and τ_2) and for solubilized rhodopsin (τ)

Temperature (°C)	τ_1 (ns)	τ_2 (ns)	τ (ns)
32	10 ± 1	110 ± 8	105 ± 7 (30°C)
25	14 ± 1	151 ± 9	n.d.
20	26 ± 3	271 ± 13	175 ± 12
17	n.d.	n.d.	220 ± 19
12	37 ± 2	293 ± 17	420 ± 25
10	45 ± 3	543 ± 35	450 ± 32
9	49 ± 5	739 ± 42	n.d.
7	57 ± 4	976 ± 51	650 ± 46
5	65 ± 6	1105 ± 67	n.d.

n.d., not determined

rhodopsin showed a different behavior (Table 1), since only one process could be observed by LIOAS, with a decay time constant comparable to the BSI → lumi transition. The general trend was that in detergent-solubilized samples the observed decay became slightly faster (see Fig. 4).

For further data analysis the activation parameters for the transitions observed were calculated from Arrhenius plots (see Fig. 4). Both apparent activation energies E_a obtained by LIOAS for washed membranes and for dodecyl-β-D-maltoside-solubilized rhodopsin (Table 2) are somewhat larger than the apparent values from absorption data with octyl-glucoside-solubilized rhodopsin (Hug et al., 1990; Horwitz et al., 1983). In the case of the washed membranes, however, the similarity further supports the assignment of τ_2 and τ_3 to the batho-to-BSI and to the BSI-to-lumi transitions, respectively. With solubilized rhodopsin, the only decay observed should be identified with the decay from BSI (equilibrated with batho within our observation time) into lumi. The lack of discrimination between batho and BSI under these conditions is probably due to a very small energy and volume difference between the two transients, i.e., a two small amplitude (Eqs. 2 and 6) of the BSI decay.

Although the preexponential factors bear a large error since they are obtained from the intercepts of the plots in Fig. 4 (Table 2), the values show a definitive trend. The observed activation energies obtained by LIOAS with rhodopsin in intact membranes are larger for both transitions and, concomitantly, the preexponential factors are also larger than those observed for solubilized membranes by

FIGURE 3 (*a* and *b*) LIOAS signal for a solution of (*curve 2*) rhodopsin-containing membranes in Ringer's solution (pH 7.0, A_{500} = 0.5, corrected for scattering), and (*curve 1*) the reference BCP in the same buffer with added washed membranes, and (*curve 3*) simulated convoluted signal; λ_{exc} = 500 nm. (*a*) PZT detector, T = 10°C; (*b*) PVF_2 detector, T = 25°C. The distribution of residuals between the simulated (tri and biexponential functions fitted in upper and lower distributions, respectively) and the measured signals are depicted. (*c*) LIOAS signal for a Ringer's solution of (*curve 2*) rhodopsin and dodecyl-β-D-maltoside (pH 7.0, A_{500} = 0.3, 17°C) and (*curve 1*) the reference Evans blue in the same solution, and (*curve 3*) simulated convoluted signal; λ_{exc} = 500 nm (single, bi, and triexponential functions fitted in the three distributions. Note that no improvement is obtained from bi to triexponential fitting).

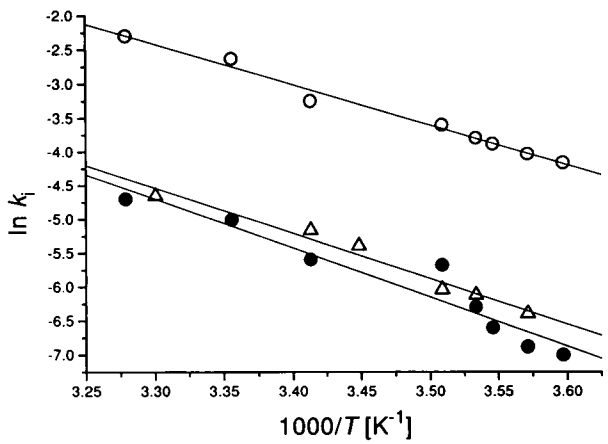

FIGURE 4 Arrhenius plots for the decay time constants of the second (batho → BSI, ○) and third component (BSI → lumi, ●) of the LIOAS fitting function for washed membranes and (△) for the decay of the second component (BSI → lumi) of the LIOAS fitting function for dodecyl-β-D-maltoside-solubilized rhodopsin. The ordinate values are given for rate constants in ns^{-1}.

Hug et al. (1990) (the comparison is made with the *observed* rate constants by these authors). For the transition assigned to BSI → lumi, the values in the membrane are also larger than our own for solubilized rhodopsin. This indicates that the transitions 1) probably imply protein regions which interact with the lipids in the membranes and are affected by the detergent, 2) are mostly under entropic control since a relatively small perturbation in the value of E_a is compensated by a variation in the preexponential factor (Dunitz, 1995), and 3) they imply that in the case of solubilized pigment less bond breaking is necessary to reach the transition state (and therefore less activation entropy) than in the case of the membrane-bound pigment [these bonds are most probably hydrogen bridges (Dunitz, 1995)]. This indicates that the membrane surrounding provides a conformational rigidity which keeps the conformational changes on a predefined pathway, also at the level of the early stages in the phototransformation.

TABLE 2 Arrhenius activation parameters (activation energy, E_a, and preexponential factor, A) for the indicated observed decay rate constants in the range 5–32°C, obtained by LIOAS after excitation of rhodopsin in the indicated medium

	k_1	k_2
Method and Medium	E_a (kJ/mol) A (s^{-1})	E_a (kJ/mol) A (s^{-1})
LIOAS	49 ± 2.3	60 ± 6
washed membranes	2.9×10^{16}	2.2×10^{17}
LIOAS	not found	57 ± 5
solubilized rhodopsin		8×10^{16}
absorption	44*	51 ± 4*#
spectroscopy	2.3×10^{15}*	6.6×10^{15}*,#

Literature values from absorption spectroscopy are included for comparison.
*Hug et al. (1990), values obtained for detergent-solubilized rhodopsin.
#Values also obtained by Horwitz et al. (1983) for washed membranes and for solubilized rhodopsin.

As already discussed in the literature for other protein reactions (Beece et al., 1981; Karplus and MacCammon, 1983; Lindemann et al., 1993) the very large values for the preexponential factors for both transitions in the intact membrane (Table 2) cannot be explained by using the arguments for diffusion-controlled solvent-dependent processes. To explain these large A factors, Beece et al. (1981) proposed a modified Arrhenius equation where the preexponential term is defined as a product of several factors, taking into account the interaction of the co-factor and the protein with the environment. Briefly, a larger A factor implies a more rigid environment, while a lower A factor implies a more flexible surrounding of the region undergoing transformation. According to our data, detergent would thus perturb the rigid protein regions transformed during the batho → BSI and the BSI → lumi transitions. Obviously, the batho ⇄ BSI equilibrium is also perturbed by the detergent in such a manner that LIOAS, which follows the heat release and structural volume changes, cannot detect the individual transients as it could for rhodopsin in the membrane.

Analysis of the amplitudes

To determine the enthalpy change in each step it is necessary to have a proper separation of the two first terms (rhodopsin → batho and batho → BSI) at every temperature. In the case of the washed membranes, the high noise of the signal, especially at the lower temperatures, impaired a good separation of the amplitudes of the two components with shorter lifetimes. This problem has already been discussed by Norris and Peters (1993). The insufficient separation of both amplitudes leads to an underestimation of the amplitude corresponding to the formation of batho and, consequently, to an overestimation of the contribution of the batho to BSI decay. Thus, for the quantitative analysis at all temperatures, the two first amplitudes were treated as a sum. The preexponential factor φ_{1+2} corresponds to the transition rhodopsin → BSI (derived from the fitting program using Eqs. 3–5).

We have chosen a simple sequential mechanism to analyze the data since in the case of the washed membranes there is no optical global analysis showing evidence for the presence of BSI and its equilibrium with the batho transient. In spite of the fact that our LIOAS data with washed membranes did indicate the presence of an ns intermediate, we have no precise values for the equilibrium constant between BSI and lumi in this medium. In solubilized pigment we did not find such an intermediate between batho and lumi. Unfortunately, the study documenting the presence of BSI with solubilized rhodopsin (Hug et al., 1990; Kliger and Lewis, 1995) has not been performed for the membrane-embedded pigment using the same global anal-

ysis approach. (See the special section below for a discussion of the consequences of the consideration of a batho ⇄ BSI equilibrium model).

For washed membranes, the amplitude φ_{1+2} (○) is plotted versus $c_p\rho/\beta$ (Fig. 5). The intercept of this plot gives q_{1+2}, which is used with the energy balance in Eq. 7 to calculate the enthalpy change upon transition from rhodopsin to BSI, $\Delta H_{Rh^*\text{-}BSI}$.

Equation 7 takes into account that several processes are involved, i.e., the radiationless relaxation from vibrationally excited S_1 (E_λ = 239.17 kJ/mol) to relaxed S_1 with a 0–0 energy level of 222 kJ/mol (as derived from the crossing of the absorption and the emission band; Guzzo and Pool, 1968), the internal conversion from relaxed rhodopsin S_1 to S_0, and the transformation to BSI with a quantum yield assumed to be equal to the production of lumi (0.67, Dartnall, 1972), i.e., $\Phi_b = \Phi_{batho} = 0.67$. Since fluorescence can be neglected ($\Phi_f = 10^{-5}$, Doukas et al., 1984), $\Phi_{IC} = 1 - \Phi_b$.

$$q_{1+2} = \Delta H_1 = E_\lambda - E_{0\text{-}0} + E_{0\text{-}0} \times \Phi_{IC} + \Delta H_{Rh^*\text{-}BSI} \times \Phi_b \quad (7)$$

Using the intercept of 0.76 (Fig. 5 *a*), a value $\Delta H_{Rh^*\text{-}BSI}$ = 137 ± 20 kJ/mol was calculated. With this value and E_{0-0} = 222 kJ/mol, the energy content of BSI results to be 85 ± 20 kJ/mol. Considering unity the efficiency of the process batho → BSI, i.e., Φ_{BSI} = 0.67, an expansion of 26 ± 3 ml/mol results from the slope = 0.074 ml/kJ of the line in Fig. 5 *a* (Eq. 6).

The amplitude φ (●) for the process BSI → lumi is also plotted as a function of $c_p\rho/\beta$ in Fig. 5 *a*. The intercept of this plot has a large error. The intercept is estimated as −0.004 ± 0.01 and an enthalpy change of −1 ± 5 kJ/mol results for the transition BSI → lumi, i.e., no enthalpy change is observed for this transition.

An expansion of 9 ± 3 ml/mol was calculated from the slope = 0.026 ml/kJ of the plot for φ_3 in Fig. 5.

The data with solubilized rhodopsin demonstrated a larger heat release. For the fast step, the heat release of 115 kJ/mol obtained from the intercept (0.86) of φ_1 versus $c_p\rho/\beta$ (Fig. 5 *b*) and the quantum yield of 0.67 (Dartnall, 1972) afforded an energy content of 50 ± 20 kJ/mol for the first transient. The structural volume change, calculated from the slope, using the same quantum yield is 20 ± 1 ml/mol. From the intercept of φ_2 in Fig. 5 *b*, a small heat release of 39 ± 20 kJ/mol and from the slope a structural volume change of 11 ± 2 ml/mol are obtained. Thus, the energy content of the lumi intermediate is 11 ± 20 kJ/mol in solubilized rhodopsin and the total structural volume change from rhodopsin to lumi is 31 ± 3 ml/mol. This value is, within the experimental error, similar to the total structural volume change rhodopsin → lumi of 26 + 9 ml/mol = 35 ± 6 ml/mol in washed membranes and similar also to the value determined in previous optoacoustic measurements (Marr and Peters, 1991). These authors measured an expansion of 29 ml/mol for the overall rhodopsin → lumi transition in bovine rhodopsin solubilized with dodecyl-β-D-maltoside. The method used by Marr and Peters (1991) was similar to ours. However, these authors could not detect time shifts in their signals, probably due to the large acoustic transit time, determined by their wide laser beam (see below).

The heat release estimated by Marr and Peters for the transition of rhodopsin → lumi in solubilized samples was 227.6 kJ/mol (excitation was at 500 nm), affording an energy content of only 16 ± 24 kJ/mol for lumi. This value is much smaller than our lumi enthalpy content value of 85 ± 20 kJ/mol for washed membranes and similar to 11 kJ/mol for solubilized protein.

Our enthalpy content value for lumi in the membrane is similar to the older photocalorimetric measurement for lumi such as 108.8 kJ/mol obtained at 198 K in a glycerol/water matrix (Cooper, 1981). It is plausible that the rigidity of this

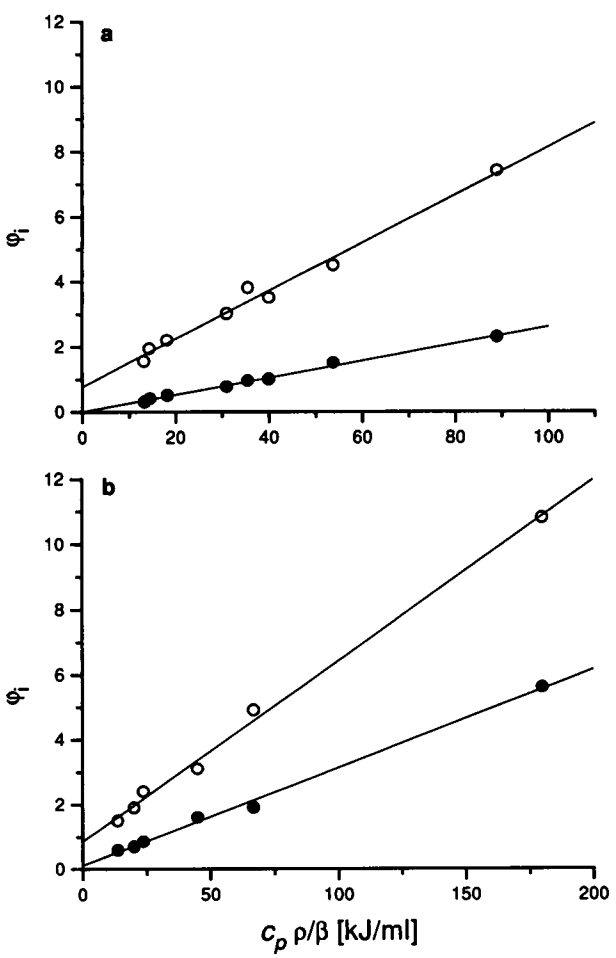

FIGURE 5 (*a*) Preexponential factors of the fitting function determined by deconvolution of the LIOAS signals for washed membranes, φ_{1+2} (○) and φ_3 (●), versus the ratio of thermoelastic parameters at various temperatures (extreme left and extreme right at 32 and 5°C, respectively). (*b*) same as (*a*) for dodecyl-β-D-maltoside-solubilized rhodopsin, φ_1 (○) and φ_2 (●).

matrix (similar to the effect of the rigid membrane environment in the washed membranes) provides a higher energy level for the lumi transient, while the detergent loosens interactions inducing relaxation to a lower level.

Consequences of the consideration of a batho ⇄ BSI equilibrium model

Hug et al. (1990) demonstrated the existence of an equilibrium batho ⇄ BSI in solubilized rhodopsin, and there are all reasons to believe that this equilibrium is also present in the washed membranes. However, as discussed above, we have no data for the temperature dependence of the equilibrium constant between batho and BSI in the membrane. The bad separation between the two shorter lifetimes in the deconvolution analysis of the LIOAS signals for the washed membranes (see above) impaired the determination of the volume changes for the individual steps rhodopsin → batho and batho → BSI. Notwithstanding this fact, the amplitude of each of the steps showed a positive trend with increasing values of $c_p\rho/\beta$, which indicates an expansion for each step (see Eq. 6). Thus, using the values determined by Hug et al. (1990) for the values of the equilibrium constant in solubilized rhodopsin, we estimate that consideration of the equilibrium would increase the slopes of the plots of φ_{1+2} (Fig. 5 *a*) and of φ_1 (Fig. 5 *b*) versus $c_p\rho/\beta$, leaving the intercepts practically unchanged. Consequently, the values of the structural volume changes $\Delta V_{R,i}$ for the processes up to BSI are lower limits and the values would be larger than those quoted for the sequential model, i.e., $(\Delta V_{Rh^*\text{-}BSI)eq} \geq (\Delta V_{Rh^*\text{-}BSI})_{seq}$. The opposite is the case for the decay of BSI to lumi, i.e., consideration of the equilibrium model would decrease the slopes of the plots of φ_3 versus $c_p\rho/\beta$ (Fig. 5 *a*) and φ_2 versus $c_p\rho/\beta$ (Fig. 5 *b*), thus decreasing the volume differences. The enthalpy difference between BSI and lumi remains almost zero (see above).

CONCLUSIONS

Temperature-dependent LIOAS measurements have been performed with rhodopsin in its native membrane surrounding, taking special precautions to handle scattering samples (silvering of the cuvette wall and determination of the thermoelastic parameters under scattering conditions). Application of signal deconvolution procedures with two different detectors and a kinetic scheme for sequential reactions allowed resolution of the photochemistry evolving from batho to the lumi formation. Lifetimes in the order of those previously assigned to the BSI transient in solubilized rhodopsin were found in the LIOAS decay analysis of the membrane-bound photoreceptor at temperatures from 5 to 32°C, thus confirming the existence of this intermediate.

The analysis of the amplitudes of the decay-fitting function in the case of the washed membranes indicates that the energy content of BSI (85 kJ/mol) is similar to that of lumi. The volume changes are an expansion of 26 ml/mol for the transition rhodopsin → BSI, and a further expansion of 9 ml/mol for the BSI → lumi transition (see Fig. 6 for a graphic summary of the values determined in this work). In dodecyl-β-D-maltoside-solubilized rhodopsin, the energy level of the first intermediate (probably batho in equilibrium with BSI) is 50 ± 20 kJ/mol and that of lumi is further decreased to 11 kJ/mol, which underlines the effect of the relatively rigid matrix environment in the native system.

Since the energy content of BSI and lumi is nearly the same, entropy should control this exergonic reaction, concomitant with the expansion of 9 ml/mol. The comparison of the activation parameters for the batho → BSI and the BSI → lumi transformations in intact membranes and in solubilized rhodopsin (from our data and from literature data), suggests that both transitions imply the breaking and reforming of weak interactions in lipophilic regions of the protein which are affected by the addition of detergent. The total volume change for the rhodopsin → lumi transition, however, is similar for both environments, i.e., 35 ± 6 ml/mol in the membrane and 31 ± 3 ml/mol in detergent. Consideration of an equilibrium model batho ⇄ BSI would increase the values of the structural volume changes be-

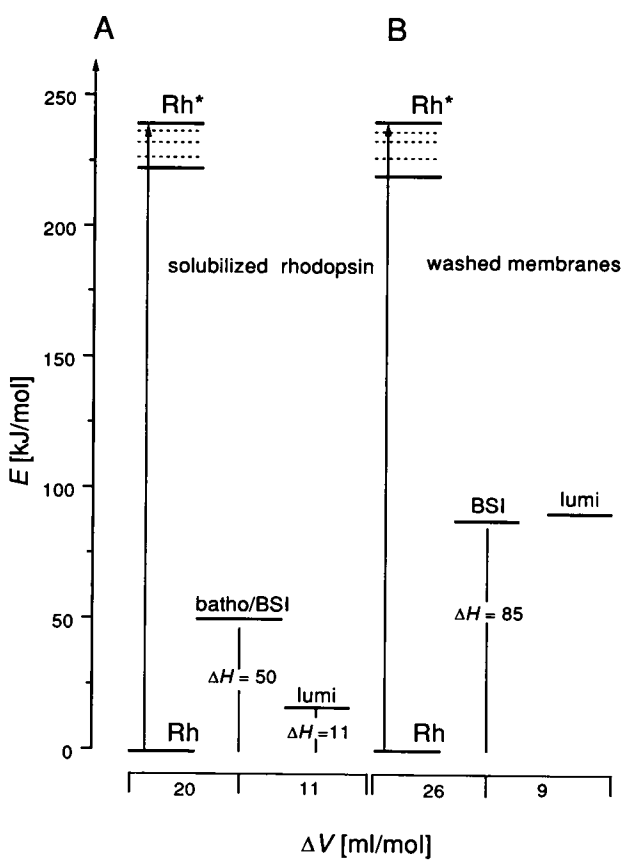

FIGURE 6 Diagram showing the energy levels of various intermediates and the structural volume changes for the various steps of the photoinduced transformation of (A) solubilized rhodopsin and (B) washed membranes. The ΔV values in ml/mol correspond to the transients as indicated and should be compared taking into account the error bars (see text).

tween batho and BSI and decrease those between BSI and lumi. The enthalpy changes would remain largely unaffected.

From a LIOAS investigation on model compounds (Churio et al., 1994) we have learned that a volume change can be explained by reorganization of the immediate environment (the solvent in these cases) upon chromophore isomerization, which results in changes in its dipole moment. In the case of complex systems such as a chromoprotein, the structural volume change should be correlated with the amino acids residues surrounding the chromophore. In fact, the relatively large changes in the orientation of the chomophore determined by time-resolved linear dichroism upon rhodopsin photolysis (for a review see Kliger and Lewis, 1995) could induce the expansions observed.

It is of obvious interest to learn, in addition to the values determined for the fastest steps of the phototransformation, about the heat release and structural volume changes occurring during the binding and activation of the G-protein, which takes place during the lifetime of metarhodopsin II in the millisecond time range. To obtain these volume changes, photothermal beam deflection (PBD) measurements, able to analyze longer time ranges than LIOAS, should be performed with rhodopsin in a similar manner as carried out with bacteriorhodopsin (Schulenberg et al., 1995). Unfortunately, preliminary PBD data with rhodopsin indicate that the scattering of the suspensions of washed membranes impairs the measurements. The PBD signal determined from the deflection of a CW laser by the photoinduced gradient of the refractive index in the solution obtained with the calorimetric reference in bleached washed membranes was already much smaller than that in a transparent buffer.

We are indebted to Professor Kurt Schaffner for his interest and generous support and to Professor Klaus Peter Hofmann (Berlin) for his advice for the rhodopsin extraction procedure. We are grateful to Dagmar Lenk, Tanja Huestege, Sigi Pörting, and Marcus Lemke for their able technical assistance, to Cristiano Viappiani for his help with the deconvolution programs, to Thomas Gensch and Peter Schmidt for valuable discussions, and to Bernd Spliethoff for the silvering of the cuvette.

REFERENCES

Applebury, M. L., D. M. Zuckerman, A. A. Lamola, and T. M. Jovin. 1974. Rhodopsin. Purification and recombination with phospholipids assayed by the metarhodopsin I to metarhodopsin II transition. *Biochemistry.* 13:3448–3458.

Baldwin, J. M. 1993. The probable arrangement of the helices in G-protein-coupled receptors. *EMBO J.* 12:1693–1703.

Beece, D., S. F. Bowne, J. Czege, L. Eisenstein, H. Frauenfelder, D. Good, M. C. Marden, J. Marque, P. Ormos, L. Reinisch, and K. T. Yue. 1981. The effect of viscosity on the photocycle of bacteriorhodopsin. *Photochem. Photobiol.* 33:517–522.

Birge, R. R. 1990. Nature of the primary photochemical events in rhodopsin and bacteriorhodopsin. *Biochim. Biophys. Acta.* 1016:293–327.

Boucher, F., and R. M. Leblanc. 1985. Energy storage in the primary photoreaction of bovine Rhodopsin. A photoacoustic study. *Photochem. Photobiol.* 41:459–465.

Braslavsky, S. E., and G. Heibel. 1992. Time-resolved photothermal and photoacoustic methods applied to photoinduced processes in solution. *Chem. Rev.* 92:1381–1410.

Braslavsky, S. E., and K. Heihoff. 1989. Photothermal methods. *In* CRC Handbook of Organic Photochemistry. J. C. Scaiano, editor. CRC Press, Boca Raton, FL. 327–355.

Callis, J. B., W. W. Parson, and M. Gouterman. 1972. Fast changes of enthalpy and volume on flash excitation of Chromatium chromatophores. *Biochim. Biophys. Acta.* 267:348–362.

Churio, M. S., K. P. Angermund, and S. E. Braslavsky. 1994. Combination of laser-induced optoacoustic spectroscopy (LIOAS) and semiempirical calculations for the determination of molecular volume changes: the photoisomerization of carbocyanines. *J. Phys. Chem.* 98:1776–1782.

Cooper, A. 1981. Rhodopsin photoenergetics: lumirhodopsin and the complete energy profile. *FEBS Lett.* 123:324–326.

Crippa, P. R., A. Vecli, and C. Viappiani. 1994. Time-resolved photoacoustic spectroscopy: new developments of an old idea. *J. Photochem. Photobiol. B Biol.* 24:3–15.

Dartnall, H. J. A. 1972. Handbook of Sensory Physiology VII/1, Photochemistry of Vision Photosensitivity. 1972. Springer-Verlag, New York. 122 pp.

DeGrip, W. J., F. J. M. Daemen, and S. L. Bonting. 1980. Isolation and purification of bovine rhodopsin. *In* Methods in Enzymology, 67. D. B. McCormick and L. D. Wright, editors. Academic Press, New York. 301–320.

Doukas, A. G., M. R. Junnarkar, R. R. Alfano, R. H. Callender, T. Kakitani, and B. H. Honig. 1984. Fluorescence quantum yield of visual pigments: evidence for subpicosecond isomerization rates. *Proc. Natl. Acad. Sci. U.S.A.* 81:4790–4794.

Dunitz, J. D. 1995. Win some, lose some: enthalpy-entropy compensation in weak intermolecular interactions. *Chemistry and Biology.* 2:709–712.

García-Quintana, D., A. Francesch, P. Garriga, A. R. de Lera, E. Padros, and J. Manyosa. 1995. Fourier transform infrared spectroscopy indicates a major conformational rearrangement in the activation of rhodopsin. *Biophys. J.* 69:1077–1082.

Gensch, T., M. S. Churio, S. E. Braslavsky, and K. Schaffner. 1996. Primary quantum yield and volume change of phytochrome-A phototransformation determined by laser-induced optoacoustic spectroscopy (LIOAS). Photochem. Photobiol. 63:719–725.

Guzzo, A. V., and G. L. Pool. 1968. Visual pigment fluorescence. *Science.* 159:312–314.

Habib-Jiwan, J.-L., B. Wegewijs, M. T. Indelli, F. Scandola, and S. E. Braslavsky. 1995. Volume changes associated with intramolecular electron transfer during MLCT state formation. Time-resolved optoacoustic studies of ruthenium cyano complexes. *Recl. Trav. Chim. Pays-Bas.* 114:542–548.

Hargrave, P. A., H. E. Hamm, and K. P. Hofmann. 1993. Interaction of rhodopsin with the G-protein, transducin. *Bioessays.* 15:43–50.

Heihoff, K., S. E. Braslavsky, and K. Schaffner. 1987. Study of 124-kilodalton oat phytochrome photoconversions in vitro with laser-induced optoacoustic spectroscopy. *Biochemistry.* 26:1422–1427.

Hofmann, K. P., S. Jäger, and O. P. Ernst. 1995. Structure and function of activated rhodopsin. *Isr. J. Chem.* 35:339–355.

Horwitz, J. S., J. W. Lewis, M. A. Powers, and D. S. Kliger. 1983. Nanosecond laser flash photolysis of rhodopsin and isorhodopsin. *Photochem. Photobiol.* 37:181–188.

Hug, S. J., W. J. Lewis, C. M. Einterz, T. E. Thorgeirsson, and D. S. Kliger. 1990. Nanosecond photolysis of rhodopsin: evidence for a new, blue-shifted intermediate. *Biochemistry.* 29:1475–1485.

Karplus, M., and J. A. MacCammon. 1983. Dynamics of proteins: elements and function. *Annu. Rev. Biochem.* 52:263–300.

Kliger, D. S., and J. W. Lewis. 1995. Spectral and kinetic characterization of visual pigment photointermediates. *Isr. J. Chem.* 35:289–307.

König, B., W. Welte, and K. P. Hofmann. 1989. Photoactivation of rhodopsin and interaction with transducin in detergent micelles. *FEBS Lett.* 257:163–166.

Lamola, A. A., T. Yamane, and A. Zipp. 1974. Effects of detergents and high pressure upon the metarhodopsin I to metarhodopsin II equilibrium. *Biochemistry.* 13:738–745.

Lindemann, P., S. E. Braslavsky, M.-M. Cordonnier, L. H. Pratt, and K. Schaffner. 1993. Effects of bound monoclonal antibodies on the decay of the phototransformation intermediates $I_{700}^{1,2}$ from native Avena phytochrome. *Photochem. Photobiol.* 58:417–424.

Marr, K., and K. S. Peters. 1991. Photoacoustic calorimetry study of the conversion of rhodopsin and isorhodopsin to lumirhodopsin. *Biochemistry.* 30:1254–1258.

Mizukami, T., H. Kandori, Y. Shichida, A. H. Chen, F. Derguini, C. G. Caldwell, C. F. Bigge, K. Nakanishi, and T. Yoshizawa. 1993. Photoisomerization mechanism of the rhodopsin chromophore. Picosecond photolysis of pigment containing 11-*cis*-locked 8-membered ring retinal. *Proc. Natl. Acad. Sci. U.S.A.* 90:4072–4076.

Nitsch, C., S. E. Braslavsky, and G. H. Schatz. 1988. Laser-induced optoacoustic calorimetry of primary processes in isolated photosystem I and photosystem II particles. *Biochim. Biophys. Acta.* 934:201–212.

Norris, C. L., and K. S. Peters. 1993. A photoacoustic calorimetric study of horse carboxymyoglobin on the 10-nanosecond time scale. *Biophys. J.* 65:1660–1665.

Ovchinnikov, Y. A. 1982. Rhodopsin and bacteriorhodopsin: structure-function relationships. *FEBS Lett.* 148:179–191.

Palings, I., J. A. Pardoen, E. M. M. van den Berg, C. Winkel, J. Lugtenburg, and R. A. Mathies. 1987. Assignment of fingerprint vibrations in the resonance Raman spectra of rhodopsin, isorhodopsin and bathorhodopsin: implication for chromophore structure and environment. *Biochemistry.* 26:2544–2556.

Peteanu, L. A., R. W. Schoenlein, Q. Wang, R. A. Mathies, and C. V. Shank. 1993. The first step in vision occurs in femtoseconds: complete blue and red spectral studies. *Proc. Natl. Acad. Sci. U.S.A.* 90: 11762–11766.

Peters, K. S., and G. J. Snyder. 1988. Time resolved photoacoustic calorimetry: probing the energetics and dynamics of fast chemical and biochemical reactions. *Science.* 241:1053–1057.

Rothschild, K. J., and W. J. DeGrip. 1992. FTIR studies of the rhodopsin transduction mechanism. *Photobiochem. Photobiophys.* 13:245–258.

Rudzki-Small, J. 1992. Deconvolution analysis for pulsed-laser photoacoustics. *Methods Enzymol.* 210:505–521.

Schertler, G. F. X., C. Villa, and R. Henderson. 1993. Projection structure of rhodopsin. *Nature (Lond.).* 362:770–772.

Schoenlein, R. W., L. A. Peteanu, R. A. Mathies, and C. V. Shank. 1991. The first step in vision: femtosecond isomerization of rhodopsin. *Science.* 254:412–415.

Schulenberg, P., and S. E. Braslavsky. 1997. Time-resolved photothermal studies with biological supramolecular systems. *In* Progress in Photothermal and Photoacoustic Science and Technology. 3. Life and Earth Sciences. A. Mandelis and P. Hess, editors. SPIE Press, Bellingham, WA. 57–81.

Schulenberg, P. J., W. Gärtner, and S. E. Braslavsky. 1995. Time-resolved volume changes during the bacteriorhodopsin photocycle: a photothermal beam deflection study. *J. Phys. Chem.* 99:9617–9624.

Strader, C. D., T. M. Fong, M. R. Tota, D. Underwood, and R. A. F. Dixon. 1994. Structure and function of G-protein-coupled receptors. *Annu. Rev. Biochem.* 63:101–132.

van Brederode, M. E., T. Gensch, W. D. Hoff, K. J. Hellingwerf, and S. E. Braslavsky. 1995. Photoinduced volume change and energy storage associated with the early transformations of the photoactive yellow protein from *Ectothiorhodospira halophila*. *Biophys. J.* 68: 1101–1109.